EUROPHYSICS LETTERS 15 July 2000

Europhys. Lett., **51** (2), pp. 147–153 (2000)

Potential energy landscape of finite-size mean-field models for glasses

A. Crisanti[1](*) and F. Ritort[2](**)

[1] *Dipartimento di Fisica, Università di Roma "La Sapienza" and INFM Unità di Roma I - P.le Aldo Moro 2, I-00185 Roma, Italy*
[2] *Physics Department, Faculty of Physics, University of Barcelona Diagonal 647, 08028 Barcelona, Spain*

(received 14 February 2000; accepted in final form 18 May 2000)

PACS. 64.70.Pf – Glass transitions.
PACS. 75.10.Nr – Spin-glass and other random models.
PACS. 61.20.Gy – Theory and models of liquid structure.

Abstract. – We analyze the properties of the energy landscape of finite-size fully connected spin-glass models with a discontinuous transition. In the thermodynamic limit the equilibrium properties in the high-temperature phase are described by the schematic mode coupling theory of super-cooled liquids. We show that *finite-size* fully connected spin-glass models do exhibit properties typical of Lennard-Jones systems when both are near the critical glass transition, where thermodynamics is ruled by energy minima distribution. Our study opens the way to consider activated processes in real glasses through finite-size corrections (*i.e.* calculations beyond the saddle-point approximation) in mean-field spin-glass models.

In recent years a significant effort has been devoted to the understanding of glass-forming systems. Recent theoretical and numerical results clearly show that the slowing down of the dynamics is strongly connected to the potential energy landscape. The trajectory of the representative point in the configuration space can be viewed as a path in a multidimensional potential energy surface. The dynamics is therefore strongly influenced by the topography of the potential energy landscape: local minima, barriers heights, basin of attraction and other topological properties all influence the dynamics.

The potential energy surface of a super-cooled liquid contains a large number of local minima, called *inherent structures* (IS) [1], each surrounded by a *basin* defined as the set of all configurations that a local energy minimization maps onto the IS contained within it. In this picture the time evolution of the system can be divided into *intra-basin* and *inter-basin* motion. Transition from one basin to another are expected to occur differently as the temperature is varied. In particular, when the temperature is lowered down to the order of the critical Mode Coupling Theory (MCT) temperature $T_{\rm MCT}$ the two motions become well separated in time

(*) E-mail: andrea.crisanti@phys.uniroma1.it
(**) E-mail: ritort@ffn.ub.es

and the relaxation dynamics is dominated by slow thermally activated crossing of potential energy barriers between different basins [2].

The essential features of MCT for glass-forming systems are also common to some fully connected spin-glass models, called mean-field p-spin glass with $p > 2$ [3,4]. In the thermodynamic limit the high-temperature phase (paramagnetic in the spin-glass language and liquid in glass language), is described by the schematic mode MCT for super-cooled liquids [4, 5]. As a consequence at the critical temperature, called $T_{\rm D}$ in p-spin language and $T_{\rm MCT}$ in MCT language, an ergodic to non-ergodic transition takes place. In mean-field models the barriers separating different ergodic components are proportional to the system size, hence infinite in the thermodynamic limit, and at $T_{\rm D}$ the relaxation time diverges. We note that despite this strong ergodicity beaking the dynamical behaviour is far from being trivial [4,6]. In real systems the barriers are of finite height and the transition to a glassy state appears at $T_{\rm g} < T_{\rm D}$, the glass transition temperature, where the typical activation time over barriers is of the same order as the observation time.

Despite these differences mean-field models, having the clear advantage of being analytically tractable, have been used to study the phase space structure of glassy systems, especially between the dynamical temperature $T_{\rm D}$ and the static temperature $T_{\rm c}$ (Kauzmann temperature $T_{\rm K}$ in glass language) where a real thermodynamic phase transition driven by the collapse of the configurational entropy takes place. The main drawback is that, since activated processes cannot be captured by mean-field models, the picture that emerges is not complete. Let us also remark that, despite the large amount of analytical work devoted to the study of the static as well as dynamical properties in the $N \to \infty$ limit, much less is known concerning the finite-N behavior.

In this letter we investigate numerically *finite-size* fully connected spin-glass models, where activated processes are present. We find strong indications that, once activated processes are allowed, mean-field spin-glass models with a discontinuous transition [3] do exhibit properties similar to the ones recently observed in simulations of Lennard-Jones systems near $T_{\rm MCT}$ [7–10], making these systems highly valuable for studying the glass transition not only at MCT level but also in the activated regime. Although the IS approach may be generally applied to short-ranged systems, it does not necessarily describe glassy dynamics in too simple models (for a recent discussion see [11]). Furthermore, Stillinger [12] has given solid arguments why for realistic short-ranged interactions with point-like defects with respect to the amorphous reference state, a Kauzmann transition cannot exist at finite temperature. This result also holds for finite-size mean-field models.

Here we shall focus on the equilibrium properties of the Ising-spin Random Orthogonal Model (ROM) [13,14] which shows a discontinuous spin-glass transition identical to that found in p-spin models [15]. Similar results are, however, obtained using other p-spin–like models, as for example the Bernasconi Model and the Ising p-spin model. Consequently, our conclusions and results should be generally valid for mean-field spin glasses with a discontinuous transition. The advantage of the ROM lies in its interaction term which is two-body, at difference with the p-body interaction of p-spin models, making the simulations much faster. Moreover, the ROM has a very strong freezing glass transition [13] making it an extremely good microscopic realization of the Random Energy Model [16].

The model is defined by the Hamiltonian

$$H = -2 \sum_{ij} J_{ij}\, \sigma_i\, \sigma_j\,, \tag{1}$$

where $\sigma_i = \pm 1$ are N Ising spin variables, and J_{ij} is a $N \times N$ random symmetric orthogonal matrix with $J_{ii} = 0$. Numerical simulations are performed using the Monte Carlo method

with the Glauber algorithm. For $N \to \infty$ this model has the same thermodynamic properties of the p-spin model: a dynamical transition at $T_{\rm D} = 0.536$, with threshold energy per spin $e_{\rm th} = E_{\rm th}/N = -1.87$, and a static transition at $T_{\rm c} = 0.25$, with critical energy per spin $e_{\rm 1rsb} = -1.936$ [13,14].

The two transitions can be understood from a "geometrical" point of view. The TAP analysis of these models [14,17] reveals that the phase space visited is composed by an exponentially large (in N) number of different basins, separated by infinitely large (for $N \to \infty$) barriers. Different basins are unambiguously labelled by the value of the energy density e at $T = 0$. Each TAP solution describes the thermodynamics within the basins labelled by e and at $T = 0$ coincide with the potential energy local minima, *i.e.* the IS of the system. The dynamical transition is associated with IS with the largest basin of attraction for $N \to \infty$, while the static transition with IS with the lowest accessible free energy [17,18].

In the mean-field limit, the allowed values of e are between $e_{\rm 1rsb}$ and $e_{\rm th}$. Solutions with e larger than $e_{\rm th}$ are unstable [19], while solutions with e smaller than $e_{\rm 1rsb}$ have negligible statistical weight [14,17]. The IS with energy equal to the threshold energy $e_{\rm th}$ can be identified with the less stable solutions. These IS have the largest (exponentially with N) statistical weight so that a rapid cooling from an equilibrium state at $T > T_{\rm D}$ down to $T = 0$ will, with probability one for $N \to \infty$, drive the system to IS with $e = e_{\rm th}$. For finite N the scenario is different since not only IS with $e < e_{\rm th}$ acquire statistical weight, but solutions with $e > e_{\rm th}$ and few negative directions [19] may become stable, simply because there are not enough degrees of freedom to hit them.

To analyze the thermodynamics of finite systems we follow the ideas of Stillinger and Weber [20] and decompose the partition sum into a sum over different IS and a sum within each basin. Collecting all IS with the same energy e, denoting with $\exp[N s_{\rm c}(E)]\,{\rm d}e$ the number of IS with energy between e and $e + {\rm d}e$, and shifting the energy of each basin with that of the associated IS, the partition sum can be written as [20]

$$Z_N(T) \simeq \int {\rm d}e \exp\left[N\ \left[-\beta e + s_{\rm c}(e) - \beta f(\beta, e)\right]\right]\,, \tag{2}$$

where $f(\beta, e)$ can be seen as the free energy density of the system when confined in one of the basin associated with IS of energy e. The function $s_{\rm c}(e)$ is the *configurational entropy density* also called *complexity* (the same derivation can be also obtained within the replica approach [21]). From eq. (2) we easily obtain the probability that an equilibrium configuration at temperature $T = 1/\beta$ lies in a basin associated with IS of energy between e and $e + {\rm d}e$:

$$P_N(e, T) = \exp\left[N\ \left[-\beta e + s_{\rm c}(e) - \beta f(\beta, e)\right]/Z_N(T)\right]. \tag{3}$$

Taking the $N \to \infty$ limit we recover the mean-field results [13,14,17]. Here we keep N *finite*.

From the partition function we can compute the average internal energy density. This is given by $u(T) = \langle e + \partial(\beta f)/\partial\beta\rangle = \langle e(T)\rangle + \langle \Delta e(T)\rangle$, where the first term is the average energy of the IS relevant for the thermodynamics and the second is the contribution coming out from fluctuations within the IS. The average is taken with the weight (3). In the limit $N \to \infty$ the only relevant IS are those with $e = e_{\rm th}$, and $\lim_{N\to\infty}\langle e(T)\rangle = e_{\rm th}$ for any $T > T_{\rm D}$. To measure $\langle e(T)\rangle$ for finite N we consider the following experiment. First we equilibrate the system at a given temperature T, then we instantaneously quench it at $T = 0$. This is obtained by decreasing the energy along the steepest descent path. In this way we can identify the energy of the IS. The experiment is repeated several times starting from uncorrelated equilibrium configurations at T and the average IS energy is computed. In fig. 1 we report $\langle e(T)\rangle$ as a function of temperature T for system sizes $N = 48$, 300 and 1000. As expected, as N increases

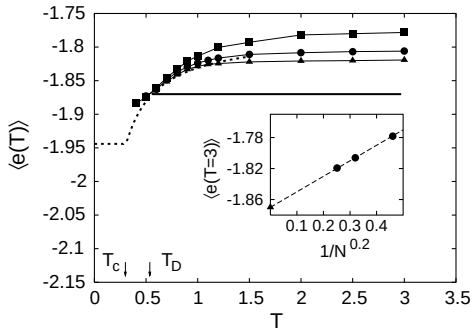

Fig. 1 – Temperature dependence of $\langle e(T)\rangle$ for $N = 48$ (square), $N = 300$ (circle) and $N = 1000$ (triangle). The average is over 10^3 different equilibrium configurations at temperature T. The horizontal line is the $N \to \infty$ limit. The arrows indicate the critical temperatures $T_{\rm D}$ and $T_{\rm c}$ (see text). The dotted line is the curve obtained from the configurational entropy for large N. In the inset the size dependence of $\langle e(T = 3)\rangle$ is shown as a function of $N^{-\alpha}$ with $\alpha = 0.2$ extrapolated down to -1.87 (triangle).

$\langle e(T)\rangle$ tends to $e_{\rm th}$. From the numerical data we found that the plateau energy approaches $e_{\rm th}$ with the power law $\langle e_{\rm plateau}\rangle - e_{\rm th} \sim N^{-0.2}$, see inset in fig. 1. Note that since N is finite we can equilibrate the system also below $T_{\rm D}$, down to the glassy transition $T_{\rm g}(N)$, ~ 0.35 for $N = 48$ and ~ 0.5 for $N = 300$, below which the system falls out of equilibrium [22].

The figure shows that for finite N and T not too close to $T_{\rm D}$ the thermodynamics is dominated by IS with $e > e_{\rm th}$. This is clearly seen from the (equilibrium) probability distribution of e since it is centered about $\langle e(T)\rangle$ indicating that IS with $e \simeq \langle e(T)\rangle$ have the largest statistical weight. This scenario has been also observed in numerical simulation of, *e.g.*, Lennard-Jones systems [7, 8, 23, 24].

In the temperature range where eq. (3) is valid, the curves $\ln P_N(e, T)+\beta e$ are equal, except for a temperature-dependent factor $\ln Z_N(T)$, to $s_{\rm c}(e)-\beta f(\beta, e)$. If we can neglect the energy dependence of $f(\beta, e)$, then it is possible to superimpose the curves for different temperatures. The resulting curve is, except for an unknown constant, the complexity $s_{\rm c}(e)$. The curves obtained for system sizes $N = 48$ and 300 and various temperatures between $T = 0.4$ and $T = 1.0$ are shown in fig. 2(a). The data collapse is rather good for $e < -1.8$. Above $e < -1.8$ the curves cannot be superimposed indicating that the energy dependence of $f(\beta, e)$ cannot be neglected anymore. In liquid language this is the anharmonic threshold [9,10]. To compare the result with the analytical predictions each curve has been translated to maximize the overlap with the theoretical prediction for $s_{\rm c}(e)$ [14]. The line is the quadratic best fit from which we can estimate the critical energy $e_{\rm c} \simeq -1.944$, where $s_{\rm c}(e_{\rm c})$ vanishes, in good agreement with the theoretical result $e_{\rm 1rsb} = -1.936$ [14].

A direct consequence of $f(\beta, e) \simeq f(\beta)$ for $e < -1.8$ is that in this range the partition function can be written as the product of an intra-basin [25] contribution ($\exp[-N\beta f]$) and of a configurational contribution which depends only on the distribution of IS energy densities. The system can then be considered as composed by two independent subsystems: the intra-basin subsystem describing the equilibrium when confined within basins, and the IS subsystem describing equilibrium via activated processes between different basins. As the temperature is lowered and/or N increased the two processes get more separated in time and the separation into two subsystems becomes more and more accurate. A similar scenario is also oserved in numerical simulations of super-cooled liquids, such as Lennard-Jones systems, near the

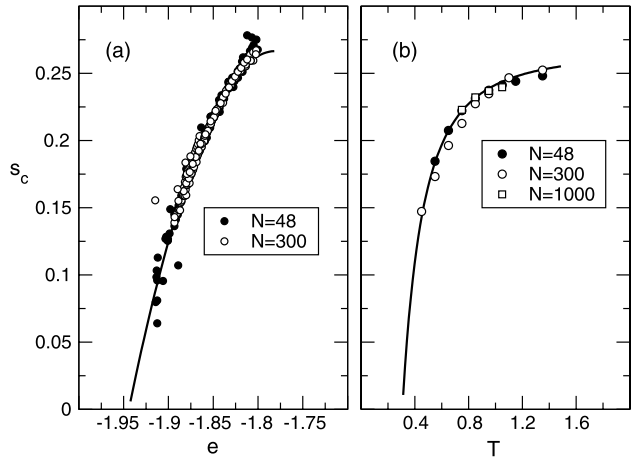

Fig. 2 – (a) Configurational entropy as a function of energy. The data are from system sizes $N = 48$ and $N = 300$, and temperatures $T = 0.4$, 0.5, 0.6, 0.7, 0.8, 0.9 and 1.0. For each curve the unknown constant has been fixed to maximize the overlap between the data and the theoretical result [14]. The line is the quadratic best fit. (b) Configurational entropy density as a function of temperature. The line is the result from the best fit of $s_c(e)$, while the symbols are the results from the temperature integration of eq. (5) for $N = 48$, $N = 300$ and $N = 1000$.

MCT transition [2, 26]. The form of $f(\beta)$ for the specific system can be computed studying the motion near the IS, for example using a harmonic approximation [9, 10]. However, this usually gives only a small corrections to thermodynamic quantities for T close to $T_{\rm D}$ [9, 10] and we do not consider it in this letter.

Another important consequence of the separation into two subsystems is that in eq. (3) $f(\beta, e)$ can be neglected since it cancels with the equal term coming from the denominator. Therefore from the knowledge of $s_c(e)$ we can easily compute the average IS energy density

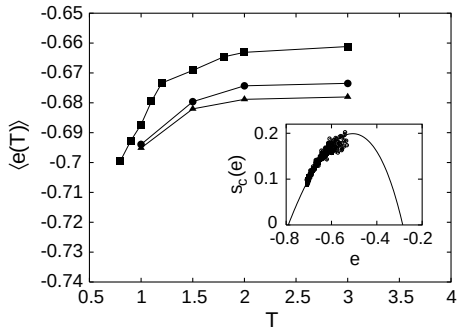

Fig. 3 – Temperature dependence of $\langle e(T)\rangle$ for the $\pm J$ SK model and $N = 192$ (square), $N = 320$ (circle) and $N = 640$ (triangle). The average is over 10^3 different equilibrium configurations at temperature T. Inset: Configuration entropy as a function of energy for the $\pm J$ SK model. The data are from system sizes $N = 64$ (circle) and $N = 192$ (square), and temperatures $T = 0.8$, 0.9, 1.0, 1.1, 1.2, 1.3. For each curve the unknown constant has been fixed to maximize the overlap between the data and the theoretical result (continuous line) [27].

$\langle e(T)\rangle$. For large N this is given by the saddle-point estimate, see eq. (3):

$$\max_e \left[-\beta\, e + s_{\rm c}(e)\right]. \tag{4}$$

The result obtained using for $s_{\rm c}(e)$ the quadratic best fit is the dotted line shown in fig. 1. The agreement with the direct numerical data is good already for $N = 300$. From the form of $\langle e(T)\rangle$ for large N we can identify the static critical temperature $T_{\rm c} \simeq 0.3$ as the temperature below which $\langle e(T)\rangle$ remains constant, not far from the theoretical results $T_{\rm c} = 0.25$ [14]. To have a check of our results we have computed the configurational entropy density using a different approach [9]. When the IS subsystem is in thermal equilibrium then the temperature dependence of the configurational entropy density can be evaluated from the thermodynamic relation

$$\frac{{\rm d}\, s_{\rm c}(T)}{{\rm d}\,\langle e(T)\rangle} = \frac{1}{T}\,, \tag{5}$$

integrating the T-dependence of ${\rm d}\,\langle e(T)\rangle/T$. Using the data of fig. 1 we obtain the curves shown in fig. 2(b). The line is the result valid for large N obtained from the quadratic best fit of $s_{\rm c}(e)$. The agreement for $N = 300$ and 1000 is rather good. We note that increasing N reduces the IS energy range explored by the system for a given fixed Monte Carlo simulation length, and this in turn reduces the temperature range in fig. 2(b). In general to have a good resolution of the IS energy range N should not be too large, however it cannot be too small to have a good sampling of the relevant IS. The sizes reported here give reasonable results, even if $N = 48$ and $N = 1000$ are close to the border.

We finally note that the analysis of the IS done in this letter can be also useful for systems with different types of transition, *e.g.* the spin glass transition. In fig. 3 we show the average IS energy density $\langle e(T)\rangle$ as a function of T for different system sizes for the mean-field $\pm J$ Sherrington-Kirkpatrick model, and in the inset the configurational entropy density $s_{\rm c}(e)$. For a more detailed IS analysis for this model see ref. [28].

To summarize, in this letter we have shown that *finite-size* mean-field spin-glass models with discontinuous transition are good candidates for studying the glass transition. Our study opens the way for addressing activated processes in glasses through finite-size corrections, *i.e.*, calculations beyond the saddle-point approximation, in mean-field spin-glass models. Finite-size mean-field spin-glass models, for instance p-spin models in the spherical approximation, have the double advantage of being analytically tractable for $N \to \infty$ and easily simulated numerically for finite N, offering a good model to analyze the glass transition.

* * *

We thank C. Donati, U. Marini Bettolo and F. Sciortino for useful discussions and critical reading of the manuscript. FR has been supported by the Spanish Government through the project PB97-0971.

REFERENCES

[1] Stillinger F. H., *Science*, **267** (1995) 1935.
[2] Schrøder T. B., Sastry S., Dyre J. C. and Glotzer S. C., *J. Chem. Phys.*, **112** (2000) 9834.
[3] Kirkpatrick T. R. and Thirumalai D., *Phys. Rev. Lett.*, **58** (1987) 2091.
[4] Crisanti A., Horner H. and Sommers H. J., *Z. Phys. B*, **92** (1993) 257.
[5] Götze W., *Z. Phys. B*, **56** (1984) 139.

[6] Cugliandolo L. and Kurchan J., *Phys. Rev. Lett.*, **71** (1993) 173.
[7] Sciortino F., Sastry S. and Tartaglia P., unpublished.
[8] Kob W., Sciortino F. and Tartaglia P., *Europhys. Lett.*, **49** (2000) 590.
[9] Sciortino F., Kob W. and Tartaglia P., *Phys. Rev. Lett.*, **83** (1999) 3214.
[10] S. Büchner and Heuer A., *Phys. Rev. E*, **60** (1999) 6507.
[11] Biroli G. and Monasson R., *Europhys. Lett.*, **50** (2000) 155.
[12] Stillinger F. H., *J. Chem. Phys.*, **88** (1988) 7818.
[13] Marinari E., Parisi G. and Ritort F., *J. Phys. A*, **27** (1994) 7847.
[14] Parisi G. and Potters M., *J. Phys. A*, **28** (1995) 5267.
[15] Bouchaud J. P., Cugliandolo L. F., Kurchan J. and Mezard M., in *Spin Glasses and Random Fields*, edited by A. P. Young (World Scientific, Singapore) 1997.
[16] Derrida B., *Phys. Rev. Lett.*, **45** (1980) 79.
[17] Crisanti A. and Sommers H. J., *J. Phys. I*, **5** (1995) 805.
[18] Kirkpatrick T. R. and Wolynes P. G., *Phys. Rev. B*, **36** (1987) 8552.
[19] Cavagna A., Giardina I. and Parisi G., *Phys. Rev. B*, **57** (1998) 11251; Barrat A. and Franz S., *J. Phys. A*, **31** (1998) L119.
[20] Stillinger F. H. and Weber T. A., *Phys. Rev. A*, **25** (1982) 978.
[21] Coluzzi B., Mezard M., Parisi G. and Verrocchio P., *J. Chem. Phys.*, **111** (1999) 9039.
[22] For finite N the correlation function always decays to zero in a finite time (which can be very long) and the system reaches thermal equilibrium. However, as T is lowered down to $T_{\rm D}$ the correlation function develops a plateau which increases as T is decreased. For $N \to \infty$ the length of the plateau diverges at $T_{\rm D}$. As done for glasses, we define the glass transition temperature $T_{\rm g}$ for finite N as the temperature at which the correlation function does not decay to zero, but stays equal to the plateau value, on the longest Monte Carlo run.
[23] Ohmine I., Tanaka H. and Wolynes P. G., *J. Chem. Phys.*, **89** (1998) 5852; Tanaka H., *Nature*, **380** (1996) 328.
[24] Sastry S., Debenedetti P. G. and Stillinger F. H., *Nature*, **393** (1998) 554.
[25] The intra-basin contribution in liquid is called "vibrational" since it is associated to vibrations near the bottom of the basin.
[26] Sciortino F. and Tartaglia P., *Phys. Rev. Lett.*, **78** (1997) 2385.
[27] Bray A. J. and Moore M. A., *J. Phys. C*, **14** (1981) 1313.
[28] Coluzzi B., Marinari E., Parisi G. and Rieger H., *On the energy minima of the SK model*, cond-mat/0003287.